Proceedings of the
International Conference on Mechanical Engineering 2003
(ICME2003) 26- 28 December 2003, Dhaka, Bangladesh

ICME03-AM-14

DELAMINATION INITIATION IN FRP LAMINATED COMPOSITES UNDER LOW VELOCITY IMPACT

Manish Khandelwal [1], **D Chakraborty** [2] **and U S Dixit** [3]

[1]Assistant System Engineer, GE-ITC, Bangalore
[2]Asstt. Prof. , Mech. Engg. IIT Guwahati
[3]Asso. Prof. , Mech. Engg. IIT Guwahati

ABSTRACT

Present paper deals with a 3D finite element analysis of FRP laminated plates subjected to low velocity impact for assessing delamination initiation. Eight-nodded layered solid element has been developed for this purpose and a computer code has been developed in C for complete 3D finite element analysis of along with appropriate criteria for assessing delamination and matrix cracking at the interface due to impact. Results of the present code have been compared with existing analytical solutions for both static and dynamic cases and an excellent agreement was found. Effect of different important parameters such as impactor mass, impactor velocity and fiber orientation on the response of the has been studied and the important results are presented. Also, comparison has been made between Graphite Epoxy and Glass-Graphite Epoxy hybrid laminate for possible improvement of response to impact.

Keywords: Impact, Delamination, Matrix cracking, Finite Element, Hybrid FRP Composites .

1. INTRODUCTION

Use of FRP laminated composites has been extensive especially in the field of aerospace industries due to their inherent advantages like high strength to stiffness ratio. However, these materials are also susceptible to damages especially in case of low velocity impact, the resulting damages like matrix cracking, delamination are sub surface in nature and are not apparent. These damages cause considerable reduction in structural stiffness leading to growth of the damage and final fracture. A large number of works have already been reported in literature in this direction and some of the important works are discussed here. Sun and Chen [1] studied the impact response of initially stressed laminate using a 2D finite element analysis and reported the effects of impactor velocity, impactor mass and the initial stress on the impact response of the laminate. Chang and Wu [2] performed transient dynamic finite element analysis of laminated FRP plate subjected to impact of foreign objects and presented the stress and strain distribution through the laminate thickness during the impact. Sun and Chattopadhyay [3] studied the contact force history of a simply supported laminate with initial stress subjected to impact of a foreign object by solving a non-linear integral equation. Kim and Goo [4] studied the impact behavior of curved composite plates using penalty finite element method. Hong and Choi [5] investigated the frequency response of impact force history from modal analysis and compared the same with the natural frequency of the system where the mass of the impactor was lumped to the plate. Choi and Chang [6] developed a model for damage initiation and the extent of damage as a function of material property, laminate configuration and impactor mass. Although many works have already been reported in the direction of low velocity impact of FRP laminated plates, proper correlation of important parameters on the impact response as well as the effect of these parameters on delamination initiation is still and important area of research and the present work aims at a 3D finite element analysis of impact response of both simple and hybrid FRP laminated composites and study the effects of various parameters such as impactor mass, impactor velocity, fiber orientation on the impact response of laminated plates.

2. FINITE ELEMENT MODELING

Figure 1 shows a laminated FRP composite plate of length *l,* width *w* and thickness *h* consisting of *N* laminae of different fiber orientation, clamped at its four edges and impacted by a spherical impactor of mass *m* radius *r* with an initial velocity of *V*.

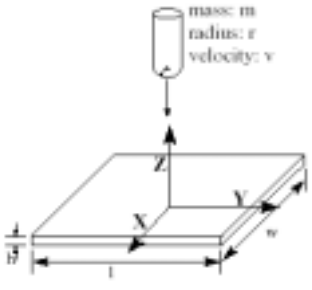

Figure 1 Impact on a laminate by spherical impactor

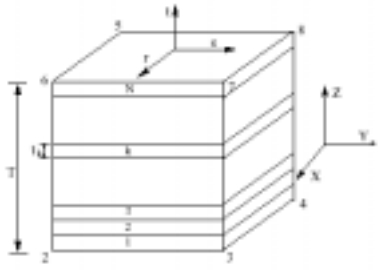

Figure 2 Eight nodded 3D layered element

2.1 8-noded layered solid element

Three dimensional 8-noded isoparametric layered solid element was used for full 3D modeling of the laminated plate (Figure 2). The shape function defining the geometry and displacement are

$$N_i = \frac{1}{8}(1+rr_i)(1+ss_i)(1+tt_i)$$
$$i = 1,2,3,...,8 \quad (1)$$

where *r, s, t* are natural coordinates and r_i, s_i, t_i are the values of natural coordinates for the i^{th} node.In order to simulate the flexural response, extra shape functions are introduced to the general 8-noded solid element and they are

$$P_1 = (1-r^2) \quad P_2 = (1-s^2) \quad P_3 = (1-t^2) \quad (2)$$

So, the displacement variation within the element is given by

$$\{d\} = \begin{Bmatrix} u \\ v \\ w \end{Bmatrix} = \sum_{i=1}^{8} N_i \begin{Bmatrix} u_i \\ v_i \\ w \end{Bmatrix} + [P]\{\Psi\} \quad (3)$$

where,

$$[P] = \begin{bmatrix} P_1 & P_2 & P_3 & 0 & 0 & 0 & 0 & 0 & 0 \\ 0 & 0 & 0 & P_1 & P_2 & P_3 & 0 & 0 & 0 \\ 0 & 0 & 0 & 0 & 0 & 0 & P_1 & P_2 & P_3 \end{bmatrix}$$

$$[\Psi]^T = \begin{bmatrix} \Psi_1 & \Psi_2 & \Psi_3 & \Psi_4 & \Psi_5 & \Psi_6 & \Psi_7 & \Psi_8 & \Psi_9 \end{bmatrix}$$

The stiffness matrix is calculated as

$$[K] = \int_{-1}^{1}\int_{-1}^{1}\int_{-1}^{1} [B]^T [C][B]|J| drdsdt \quad (4)$$

Let

$$G(r,s,t) = [B]^T [C][B]|J| \quad (5)$$

then

$$[K] = \int_{-1}^{1}\int_{-1}^{1}\int_{-1}^{1} G(r,s,t) drdsdt \quad (6)$$

For an element having *N* layers in the thickness direction (figure 2),

$$T = \sum_{k=1}^{N} t_k \quad (7)$$

where *T* is the total thickness of the element and t_k is the thickness of the k^{th} layer of the element. Taking a parameter $t \in [0,T]$ and changing the limits

$$[K] = \frac{2}{T}\int_{-1}^{1}\int_{-1}^{1}\sum_{k=1}^{N}\frac{t_k - t_{k-1}}{2}\int_{-1}^{1} F(r,s,t) drdsdt \quad (8)$$

where *t* is function of thickness over the layer.

2 x 2 x 2 Gauss quadrature scheme is applied to evaluate the above integration.

The stiffness matrix thus evaluated by equation (8) is of size 33 x 33 and includes coefficients pertaining to the incompatible modes. Using static condensation technique these terms are eliminated and the condensed stiffness matrix becomes of the order of 24 x 24 pertaining to nodal degrees of freedom only. Element mass matrix is evaluated as

$$[M^e] = \int_{V^m} [N]^T \rho [N] dv \quad (9)$$

2.2 Finite Element Contact Impact Modeling

Dynamic equation governing the impact problem (neglecting damping) is

$$[M]\{\ddot{d}\} + [K]\{d\} = \{F\} \quad (10)$$

where *[M]* and *[K]* are the mass and stiffness matrices and $\{F\}, \{d\}, \{\dot{d}\}, \{\ddot{d}\}$ are force, displacement, velocity and acceleration vectors for plate respectively. At time $t+\Delta t$, dynamic equation (10) can be written as

$$[M]\{\ddot{d}\}^{t+\Delta t} + [K]\{d\}^{t+\Delta t} = \{F\}^{t+\Delta t} \quad (11)$$

Equation (11) can be reduced to

$$[\hat{K}]\{d\}^{t+\Delta t} = \{\hat{F}\}^{t+\Delta t} \quad (12)$$

Where $[\hat{K}]$ is the effective stiffness matrix and $[\hat{F}]$ is the effective force vector and are defined as

$$[\hat{K}] = \frac{1}{\Phi \Delta t^2}[M] + [K] \quad (13)$$

$$\{\hat{F}\} = \{H\}^t + \{F\}^{t+\Delta t} \quad (14)$$

$$\{H\}^t = [M]\left(\frac{1}{\Phi \Delta t^2}\{d\}^t + \frac{1}{\Phi \Delta t}\{\dot{d}\} + \left(\frac{1}{2\Phi} - 1\right)\{\ddot{d}\}\right) \quad (15)$$

Where φ and δ are the Newmark constants.

In equation (12), displacement, velocity and acceleration

at time t are known at each point inside the plate and the unknown quantities in this equation are vector $\{d\}^{t+\Delta t}$ and the force vector $\{F\}^{t+\Delta t}$. In the absence of pre-load, (12) becomes

$$[\hat{K}]\{d\}^{t+\Delta t} = \{H\}^{t} + \{P\}^{t+\Delta t} \tag{16}$$

where $\{P\}$ is the contact force

The displacement vector $\{d\}$ is expressed as the sum of the displacements due to the force $\{H\}$ and the contact force $\{P\}$ as

$$\{d\}^{t+\Delta t} = \{d\}_{H}^{t+\Delta t} + \{d\}_{P}^{t+\Delta t} \tag{17}$$

Equations (16) and (17) give

$$[\hat{K}](\{d\}_{H}^{t+\Delta t} + \{d\}_{P}^{t+\Delta t}) = \{H\}^{t} + \{P\}^{t+\Delta t} \tag{18}$$

From equation (18) we have

$$[\hat{K}]\{d\}_{H}^{t+\Delta t} = \{H\}^{t} \tag{19}$$

and

$$[\hat{K}]\{d\}_{P}^{t+\Delta t} = \{P\}^{t+\Delta t} \tag{20}$$

At time $t+\Delta t$, contact force vector can be written as

$$\{P\}^{t+\Delta t} = f^{t+\Delta t}\{U\} \tag{21}$$

where $f^{t+\Delta t}$ is the magnitude of contact force at time $t+\Delta t$.

Equations (20) and (21) yields

$$[\hat{K}]\{d\}_{P}^{t+\Delta t} = f^{t+\Delta t}\{U\} \tag{22}$$

and for a unit contact force ($f^{t+\Delta t} = 1$)

$$[\hat{K}]\{d\}_{U}^{t+\Delta t} = \{U\} \tag{23}$$

where $\{d\}_{U}^{t+\Delta t}$ is the displacement caused by the unit contact force and

$$\{d\}_{P}^{t+\Delta t} = f^{t+\Delta t}\{d\}_{U}^{t+\Delta t} \tag{24}$$

Equations (17) and(24) give

$$\{d\}^{t+\Delta t} = \{d\}_{H}^{t+\Delta t} + f^{t+\Delta t}\{d\}_{U}^{t+\Delta t} \tag{25}$$

Using Hertzian contact law, contact force during loading and unloading are

$$f^{t+\Delta t} = \kappa(\alpha^{t+\Delta t})^{1.5} \quad \text{During Loading}$$

$$f^{t+\Delta t} = f_m\left(\frac{\alpha^{t+\Delta t} - \alpha_0}{\alpha_m - \alpha_0}\right)^{2.5} \quad \text{During Unloading} \tag{26}$$

where κ is the modified constant of the Hertz contact theory, α is the indentation depth, f_m is the maximum force just before unloading, α_m is the indentation depth corresponding to f_m and α_0 is the permanent indentation during loading and unloading process. Permanent indentation can be determined from the following expressions [2]

$$\alpha_0 = 0$$

when $\alpha_m < \alpha_{cr}$

$$\alpha_0 = \alpha_m\left[1 - \left(\frac{\alpha_{cr}}{\alpha_m}\right)^{2/5}\right] \tag{27}$$

when $\alpha_m > \alpha_{cr}$

where α_{cr} is the critical indentation. is

$$\alpha^{t+\Delta t} = \delta_S^{t+\Delta t} - \delta_C^{t+\Delta t} \tag{28}$$

Here $\delta_S^{t+\Delta t}$ is the position of the center point of the impactor and $\delta_C^{t+\Delta t}$ is the displacement of the center of the mid surface of the plate in the direction of impact. At time t+Δt, magnitude of $\delta_S^{t+\Delta t}$ can be determined by Newton's second law as

$$\delta_S^{t+\Delta t} = \int_0^{t+\Delta t} v\,dt + \int_0^{t+\Delta t}\int_0^{t+\Delta t} \frac{f}{m}\,dt\,dt \tag{29}$$

Using equation (25)

$$\delta_C^{t+\Delta t} = \delta_{CH}^{t+\Delta t} + f^{t+\Delta t}\delta_{CU}^{t+\Delta t} \tag{30}$$

Combining equations (25) – (30) the following expressions for the contact force are obtained

$$f^{t+\Delta t} = \kappa\left(\int_0^{t+\Delta t} v\,dt + \int_0^{t+\Delta t}\int_0^{t+\Delta t} \frac{f}{m}\,dt\,dt - \delta_{CH}^{t+\Delta t} - f^{t+\Delta t}\delta_{CU}^{t+\Delta t}\right)^{1.5}$$

During loading

$$f^{t+\Delta t} = f_m\left(\frac{\int_0^{t+\Delta t} v\,dt + \int_0^{t+\Delta t}\int_0^{t+\Delta t} \frac{f}{m}\,dt\,dt - \delta_{CH}^{t+\Delta t} - f^{t+\Delta t}\delta_{CU}^{t+\Delta t} - \alpha_0}{\alpha_m - \alpha_0}\right)^{2.5}$$

During Unloading

(31)

Contact force at $t+\Delta t$, i.e. $f^{t+\Delta t}$ was calculated using equation (31) (during loading or during unloading) by Newton Raphson method. From the known value of contact force $f^{t+\Delta t}$, displacement vector $\{d\}^{t+\Delta t}$ is calculated using equation (25). Once the value of $f^{t+\Delta t}$ is known, plate velocity, acceleration and then the stresses and strains at time $t+\Delta t$ was calculated. This procedure has been repeated for each time step to get the displacement, stress and strain.

2.3 Failure Criteria

2.3.1 Critical matrix cracking

In order to assess the possible matrix cracking in the laminated plate due to low velocity impact, matrix cracking criterion proposed by Choi et al[18] has been used in the present work. The criterion is expressed as

$$\left(\frac{\bar{\sigma}_{ss}^{n}}{Y^{n}}\right)^2+\left(\frac{\bar{\sigma}_{st}^{n}}{S_i^{n}}\right)^2=e_M^2$$

$e_M \geq 1 \Rightarrow failure$

$e_M < 1 \Rightarrow nofailure$

$\bar{\sigma}_{ss} \geq 0 \Rightarrow Y^n = Y_{ten}^n$

$\bar{\sigma}_{ss} < 0 \Rightarrow Y^n = Y_c^n$

where S_i is the in situ interlaminar shear strength within the laminate and Y_{ten} and Y_c are the in situ ply transverse tensile and compressive strengths respectively. $\bar{\sigma}_{ss}$ and $\bar{\sigma}_{st}$ are average in plane and interlaminar transverse stresses respectively for n^{th} ply and are expressed as

$$\bar{\sigma}_{st}^{n}=\frac{1}{h_n}\int_{t_{n-1}}^{t_n}\sigma_{st}\,dt$$

and

$$\bar{\sigma}_{ss}^{n}=\frac{1}{h_n}\int_{t_{n-1}}^{t_n}\sigma_{ss}\,dt$$

where t_n and t_{n-1} are upper and lower interfaces of n^{th} ply in the laminate and h_n is the thickness of the ply.

2.3.2 Delamination at the interface

In order to assess delamination initiation at the interface of the laminate, the criterion proposed by Choi and Chang [6] for impact induced delamination has been used in the present work. The criterion is

$$D_a\left(\frac{\bar{\sigma}_{st}^{n}}{S_i^{n}}+\frac{\bar{\sigma}_{rt}^{n+1}}{S_i^{n+1}}+\frac{\bar{\sigma}_{ss}^{n+1}}{Y^{n+1}}\right)^2=e_D^2$$

$e_D \geq 1 \Rightarrow failure$

$e_D < 1 \Rightarrow nofailure$

$\bar{\sigma}_{ss} \geq 0 \Rightarrow Y^{n+1} = Y_{ten}^{n+1}$

$\bar{\sigma}_{ss} < 0 \Rightarrow Y^{n+1} = Y_c^{n+1}$

and D_a is an empirical constant determined from experiment and $\bar{\sigma}_{rt}$ is average interlaminar longitudinal stress in the interface between n^{th} and $n+1^{th}$ ply respectively and are expressed as

$$\bar{\sigma}_{rt}^{n+1}=\frac{1}{h_{n+1}}\int_{t_{n-1}}^{t_n}\sigma_{rt}\,dt$$

3. RESULTS AND DISCUSSION

3.1 Computer Code and Validation

Based on the analytical model described above, a computer code has been developed in C language. In order to verify the FE code developed, the following parameters were used for a steel ball impacting at the center of an isotropic plate. Plate dimension: 0.2 x 0.2 x 0.008 m with all four edges clamped; Impactor (steel ball) diameter: 0.02 m; Velocity of the impactor : 1 m/s; Steel properties: E=200 x 10^9 N/m^2, ν = 0.25, G = 76.9 x 10^9 N/m^2, α_{cr} = 0.0001 m, *Density* = 7840 Kg/m^3 . The numerical solutions from the present code (with a mesh size of 12 x 12 x 2 and a time step of integration Δt = 1 μs) for contact force, displacement, velocity of the center of the plate and of the impactor have been presented in figure 3(a) – 3(c) and an excellent agreement has been observed with existing analytical solution of Karas [7].

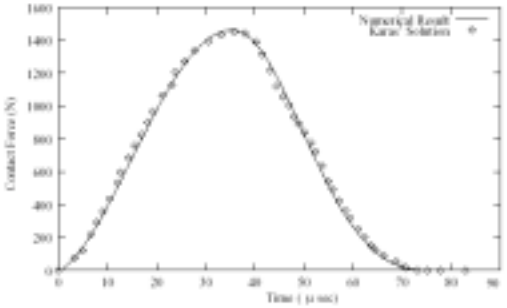

(a)

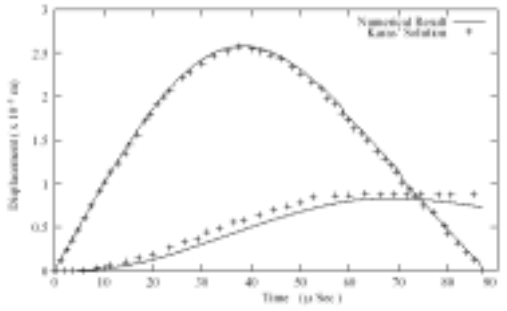

(b)

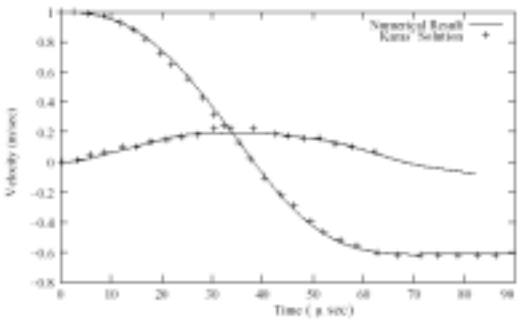

(c)

Figure 3. Impact of a steel ball on a steel plate. (a)

Contact force history (b) Displacement history (c) Velocity history

3.2 Effect of velocity on contact force history

Figure 4 shows the contact force history for an aluminum impactor on a $[0/-45/45/90]_{2s}$ Graphite/Epoxy laminate at different impactor velocities. The same trend also been observed for $[0_{Gl}/-45_{Gr}/45_{Gr}/90_{Gl}]_{2s}$ Glass-Graphite hybrid laminates. In both the cases, contact force magnitude increases with the impactor velocity.

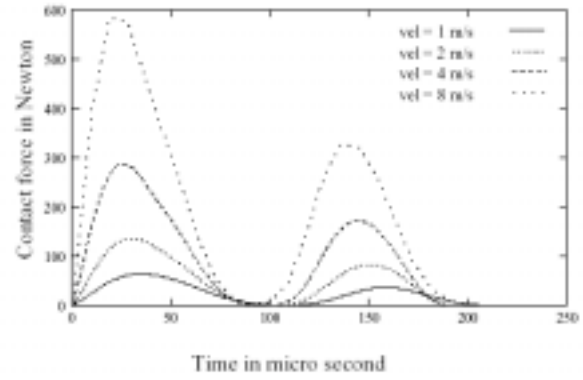

Figure 4 Contact force histories for $[0/-45/45/90]_{2s}$ Graphite/Epoxy for different impactor velocities

3.3 Effect of impactor mass on contact force history

Figures 5 shows the contact force histories for increasing impactor mass (m, 2m, 4m and 8m) for an impactor velocity of 1 m/s for $[0/-45/45/90]_{2s}$ Graphite/Epoxy. It has been observed that when the mass of the impactor increases, not only the magnitude of the contact force increases but also the contact period is prolonged. The same trend has also been observed for $[0_{Gl}/-45_{Gr}/45_{Gr}/90_{Gl}]_{2s}$ Glass-Graphite hybrid laminate.

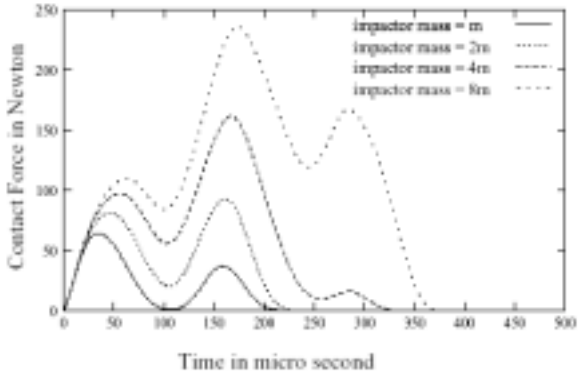

Figure 5 Contact force histories for $[0/-45/45/90]_{2s}$ Graphite/Epoxy for different impactor masses

3.4 Effect of ply orientation

Figure 6 shows the contact force histories for different values of θ (15^0, 30^0 ,45^0 , 60^0 ,75^0) in a $[0/ -\theta / +\theta /90]_{2s}$ Graphite/Epoxy laminate. It has been observed that contact force magnitude does not change much with the change in fiber orientation at the interface. The same trend has also been observed for $[0_{Gl}/-45_{Gr}/45_{Gr}/90_{Gl}]_{2s}$ Glass-Graphite hybrid laminate. Also, it has been observed that the direction of delamination initiation at the interface depends largely on the fiber orientation at the interface. In the case of $[0/-45/45/90]_{2s}$ Graphite Epoxy laminate the delamination initiates in the interface of +45/-45 and proceeds at 45^0 .

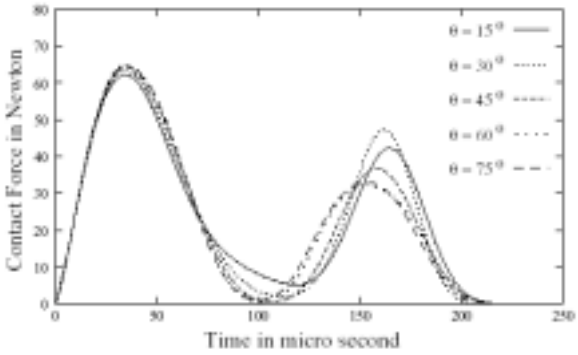

Figure 6 Contact force histories for $[0/ -\theta / +\theta /90]_{2s}$ Graphite/Epoxy for different values of θ

3.5 Effect of hybridization

Figure 7 shows the contact force histories for $[0/-45/45/90]_{2s}$ Graphite Epoxy and $[0_{Gl}/-45_{Gr}/45_{Gr}/90_{Gl}]_{2s}$ Glass-Graphite hybrid laminate for impactor velocity = 8 m/s. It could be observed that contact force magnitudes are different in two cases. Also, in the case of hybrid laminate, reloading starts late compared to Graphite Epoxy laminate. So, in case of hybrid laminate, cumulative damage will be delayed compared to that in case of Graphite Epoxy laminates and will have more life.

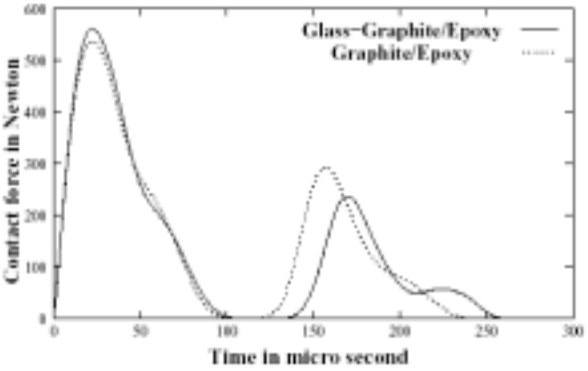

Figure 7 Contact force histories for $[0/ -\theta / +\theta /90]_{2s}$ Graphite/Epoxy and $[0_{Gl}/-45_{Gr}/45_{Gr}/90_{Gl}]_{2s}$ Glass-Graphite hybrid laminate

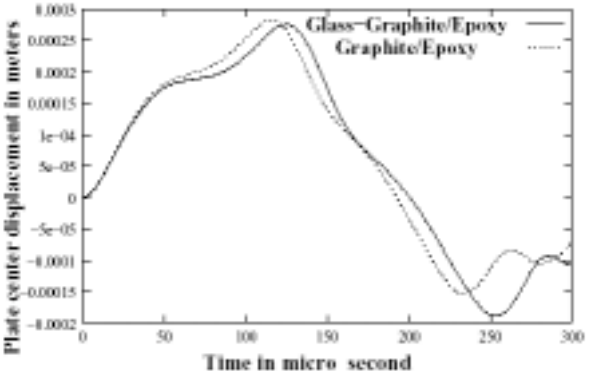

Figure 8 Plate center displacement for $[0/ -\theta / +\theta /90]_{2s}$ Graphite/Epoxy and $[0_{Gl}/-45_{Gr}/45_{Gr}/90_{Gl}]_{2s}$ Glass-Graphite hybrid laminate

Figure 8 shows the plate center displacement for

$[0/-45/45/90]_{2s}$ Graphite Epoxy and $[0_{Gl}/-45_{Gr}/45_{Gr}/90_{Gl}]_{2s}$ Glass-Graphite hybrid laminate for impactor velocity = 8 m/s. Maximum plate defection is almost same in both the cases but they occur at different time. Figures 9(a-c) show the stress histories (only σ_{zz} , τ_{yz} and τ_{xz} are shown because these are the stresses responsible for delamination at the interface) for $[0/-45/45/90]_{2s}$ Graphite Epoxy and $[0_{Gl}/-45_{Gr}/45_{Gr}/90_{Gl}]_{2s}$ Glass-Graphite hybrid laminate for impactor velocity = 8 m/s. In both the cases, magnitudes of stresses are very high indicating the chance of delamination initiation.

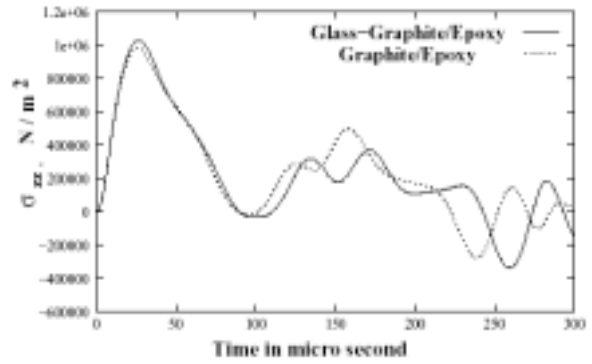

(a)

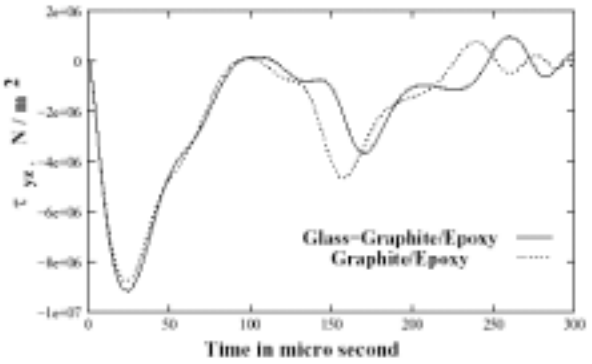

(b)

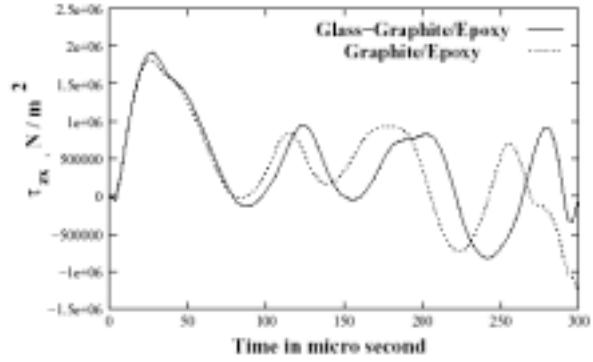

(c)

Figure 9 Stress history at location (0.036758 m, 0.036758 m, 0.001236 m) for Graphite/Epoxy and Glass-Graphite hybrid laminate (a) σ_{zz} (b) τ_{yz} (f) τ_{zx}

3.6 Delamination initiation

In all the cases, based on the criteria discussed in earlier sections, location of matrix cracking and subsequent delamination has been determined. Depending upon the magnitude of contact force (which varies with impactor velocity, impactor mass), delamination starts at various instant of time. For example in the case of $0/-45/45/90]_{2s}$ Graphite Epoxy with impactor velocity of 8 m/s, delamination starts at 1st micro second and it initiates at $+45^0/-45^0$ interface near the contact point and the same proceeds at 45^0 angle. However in the case of other ply orientation at the interface, delamination direction was observed to be different. Thus, ply orientation at the interface dictates the direction in which the delamination grows.

4. CONCLUSIONS

A 3D finite element code was developed for complete analysis of static as well as impact analysis of laminated composite plate and is capable of calculating the contact force, stress and strain history at any point of interest in the plate. Also, the code can determine the location of possible delamination and matrix cracking. From the simulation run of the code the following observations have been made.

(1) Contact force magnitude increases with increased impactor velocity as well as impactor mass as expected.
(2) In case of increased impactor mass, the contact period is prolonged.
(3) Changing the ply angle at the interface does not affect the contact force magnitude significantly but the contact period changes little bit.
(4) In case of Glass-Graphite hybrid laminate, reloading is delayed compared to that in case of Graphite epoxy laminate. Also during reloading the magnitude of contact force is less.
(5) Direction of delamination at the interface is dictated by the fiber orientation at the interface.

6. REFERENCES

1. Sun C. T. and Chen J. K., 1985,` "On the Impact of Initially Stressed Composite Laminates" Journal of Composite Materials, 19:490-504.
2. Wu H.-Yung T. and Chang F. K., 1989, "Transient Dynamic Analysis of Laminated Composite Plate Subjected to Transverse Impact",Computers & Structures, 31(3):453-466
3. Sun C. T. and Chattopadhyay S.,1975, "Dynamic Response of Anisotropic Laminated Plates Under Initial Stress to Impact of a Mass",Journal of Applied Mechanics,42:693-698.
4. Goo N. S. and Kim S. J., 1997, "Dynamic Contact Analysis of Laminated Composite Plates Under Low-Velocity Impact", AIAA Journal, 35(9): 1518-1521
5. Choi I. H. and Hong C. S., 1994, "New Approach for Simple Prediction of Impact Force History on Composite Laminates", AIAA Journal, 32(10): 2067-2072.
6. Choi H. Y. and Chang F. K., 1992, "A Model for Predicting Damage in Graphite/Epoxy Laminated Composite resulting from Low-Velocity Point Impact", Journal of Composite Materials, 26(14): 2134-2169.
7. Karas, K., 1939,``Platten unter seitchem stoss", Ingenieur Archiv. 10: 237-250.